

- 1 -

IRON PRECIPITATION KINETICS IN SYNTHETIC ACID MINE DRAINAGE

by

Harry R. Diz*¹

John T. Novak²

J. Donald Rimstidt³

ABSTRACT

To evaluate the design and operation of a new active treatment system for acid mine drainage (AMD), the behavior of ferric iron solutions after the addition of bicarbonate ions was investigated. The effects of various other factors common to AMD on the precipitation rate of iron were also studied. It was found that the rate of Fe III precipitation in synthetic AMD was not affected by the presence of Al or Mn, within the concentration ranges investigated (for Al, 0-0.01 M, for Mn, 0-0.002 M). Our experiments showed that the induction time (t_{ind}), *i.e.*, the time elapsed between the addition of base ions and the detection of iron precipitation, decreased with increasing iron concentration and pH but increased with increasing sulfate concentration:

$$\log t_{ind} = 6.7(\pm 0.30) - 1.29(\pm 0.10) \text{pH} + 0.94(\pm 0.07) \log [\text{SO}_4] - 0.36(\pm 0.05) \log [\text{Fe}]$$

Our results suggested that sulfate sorbed to the surface of growing iron oxyhydroxides, inhibiting their growth. This effect offers an important tool that can be used to control the precipitation of iron in AMD treatment facilities.

INTRODUCTION

Acid mine drainage (AMD) from working and abandoned mines continues to be an important pollution problem in the United States and around the world. Typically, AMD is high in iron, aluminum, manganese and sulfate. The pH of these waters is often less than 3. The impacts of AMD on aquatic organisms are well known (Newman and McIntosh, 1991), and the presence of metals and sulfate in natural water bodies can reduce their usefulness as water supplies. A key factor in ameliorating these effects is the removal of iron, for once the iron is removed, the acidity can be easily neutralized. Thus, the design and operation of treatment systems requires an understanding of the factors that control the rate of iron precipitation.

The degree of hydrolysis of ferric ions in aqueous solution is a function of pH. As pH increases, protons are lost from waters of hydration in a step-wise fashion. Monomers tend to form polymers by formation of Fe-OH-Fe bonds (olation), followed by formation of Fe-O-Fe bonds (oxolation) (Stumm and Morgan, 1981). Figure 1, produced using the geochemical computer program MINTQA2 (Allison et al, 1991), illustrates the increase in dimers and trimers with increasing pH.

* Corresponding author: (814) 871-7633; FAX (814) 871-7382; email: diz@gannon.edu.

¹ Dept of Environmental Science & Engineering, Gannon University, Erie, PA 16541;

² Charles E. Via Dept of Civil & Environmental Engineering,

³ Dept of Geological Sciences, Virginia Polytechnic Institute & State University, Blacksburg, Virginia 24061.

- 2 -

Above pH 3.5, the trimer $\text{Fe}_3(\text{OH})_4^{5+}$ becomes the predominant species, followed in abundance by the monomers $\text{Fe}(\text{OH})_2^+$ and FeOH^{2+} .

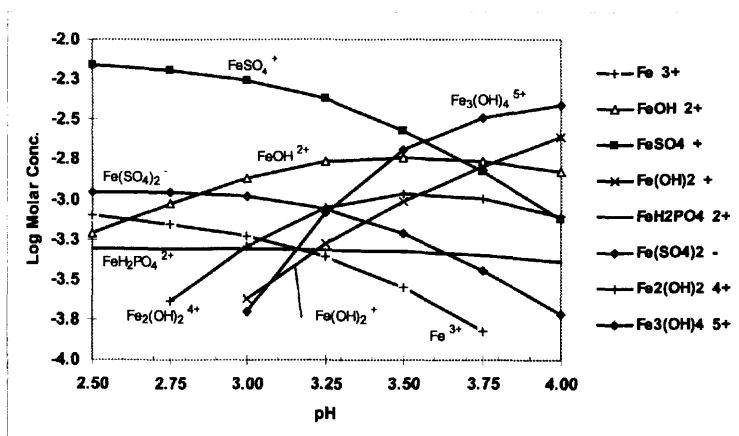


Figure 1. Relative abundance of species in a 10 mM FeT synthetic AMD solution as a function of pH. Speciation computed by MINTEQA2 (Allison et al, 1991). No solids were allowed to form.

Dousma et al. (1979) observed a delay in the iron polymerization process with increasing SO_4/Fe ratio below pH 2. They suggested that this was the result of the presence of iron-sulfate complexes. The effect of sulfate on induction times, *i.e.*, the time from the addition of the base to the appearance of a precipitate, was not reported. Parfitt and Smart (1978) provided evidence that sulfate was adsorbed onto hydrous ferric oxide (HFO) surfaces by formation of a binuclear bridge. The sulfate ion displaces the hydroxyl and protonated hydroxyl groups forming the $\equiv\text{Fe}-\text{O}-\text{S}(\text{O})_2-\text{O}-\text{Fe}\equiv$ complex (\equiv denotes surface incorporated), releasing OH^- and H_2O .

When base is added to an acidic ferric iron solution, the induction time may range from seconds to months (Dousma and de Bruyn, 1976). Van der Woude and de Bruyn (1983) postulated that induction time and subsequent nucleation was dependent on the formation of a supercritical nucleus upon the addition of a trimer to a critical-sized polymer:



Once critical size is achieved, the nuclei continue to grow by incorporation of additional Fe/OH growth units until the concentration of dissolved iron (*i.e.*, sub-critical polymers) becomes so low that the particle growth rate slows appreciably. Collision of independent particles may result in agglomeration. Agglomeration proceeds until the particle concentration per unit volume decreases to such a low level that growth by agglomeration is counter-balanced by particle

- 3 -

break-up. The appearance of a precipitate is a function of the number and size of agglomerated particles. The induction time is generally defined as that length of time from the addition of a reagent or change in conditions until the time of the detection of a precipitate (van der Woude and de Bruyn, 1983). The total induction time (t_{ind}) is in fact the sum of the time required to create stable nuclei (t_i) and the time required for the stable nuclei to grow (t_g) to sufficient size to produce a measured effect (Sohnel and Garside, 1992).

OBJECTIVES

The ease of separation of solids from water is largely a function of particle size. When iron precipitates rapidly, very small particles are formed, requiring large sedimentation basins to effect solid/water separation. The iron hydroxide sludge formed remains high in water content, making handling and disposal costly. It seems desirable to search for a technique to avoid the formation of typical gelatinous iron precipitates. Such an effort was described in another phase of this work (Diz and Novak, 1998), in which iron solutions and bicarbonate solutions were introduced to a fluidized bed reactor containing quartz sand. It was observed that very small iron particles ($< 1 \mu\text{m}$) attached to the sand grains and did not produce the gelatinous precipitate typical of more conventional treatment systems. The optimal removal of iron from solution in that system appeared to require a balance between minimizing effluent dissolved iron while slowing precipitate formation rate. This paper reports on factors thought to affect the rate at which iron precipitates formed in synthetic AMD. Conductivity and pH were measured prior to and after the appearance of turbidity in the solutions. These observations provide an insight into changes occurring in solution prior to the formation of a visible precipitate and led to the formation of certain conclusions about the mechanisms involved.

EXPERIMENTAL SECTION

Chemicals, Water and Synthetic AMD

The recipe for synthetic AMD (Table 1) was based on the USEPA findings for acid-generating coal mining activities (USEPA, 1976). All chemicals used to prepare solutions were reagent grade except for aluminum sulfate, which was technical grade. Solutions were made with deionized water, and were not filtered prior to use. Acids such as nitric, sulfuric and hydrochloric were "Plus" grade by Fisher Chemical Company.

pH Probe Response and Calibration

The response time of the pH probe/meter (Accumet AP10) was about 10 s when the probe was immersed in dilute sulfuric acid or an acidic ferric sulfate solution. The probe/meter were calibrated before each set of trials and checked during each session with pH buffers (pH 2.0, 4.0, and 7.0).

Kinetics and Induction Time Studies

Several trials were conducted by adding a bicarbonate solution to a pH 2.0 sulfuric acid solution, in which the resultant pH ranged from 2.5 to 6.0. The pH reading stabilized within 10 s. Thus,

- 4 -

the kinetics of bicarbonate/acid neutralization were deemed to be faster than the response time of the probe.

Table 1. Synthetic AMD. Concentrations shown are after addition of sulfuric acid to produce pH ~2.3. To prepare the bicarbonate solution used for neutralization, iron was omitted and sulfate was supplied as sodium sulfate instead of sulfuric acid.

Constituent	Molarity	mg L ⁻¹
Iron	0.001 - 0.010	56 - 558
Aluminum	0 - 0.002	0 - 54
Manganese	0 - 0.002	0 - 110
Calcium	0.002	80
Magnesium	0.001	24
Sodium	0.0075	175
Potassium	0.0005	20
Ammonium (as N)	0.0005	7
Sulfate	0.0015 - 0.025	144 - 2400
Phosphate (as P)	0.0005	16

Initial trials were conducted in 1 mM ferric solutions with combinations of aluminum (Al [III]), manganese (Mn [II]), and sulfate as indicated in Table 2. Later, more extensive trials were conducted to study the effect of Al, sulfate, and iron concentration on induction time (Table 3). Ten mL of iron solution (at double the desired concentration) was placed in a 100 mL beaker and 10 mL of a sodium bicarbonate solution was added quickly by syringe while the contents of the beaker were rapidly mixed by magnetic stir bar. Immediately, the solution was recirculated through the optical cell of a spectrophotometer (Beckman DU-640) for 30 s, leaving a representative sample in the cell. The solution pH at $t = 10$ s (pH_{10}) was noted and recorded. The spectrophotometer measured absorbance at 650 nm every second for 10 min. A 10 mM ferric sulfate solution absorbed strongly below 400 nm, but was essentially transparent above that wavelength, even with increase in pH. Thus, any increase in absorbance was taken to be due to particulate scattering. The end of the induction time (t_{ind}) was defined as that moment when the absorbance increased by at least $0.00005 \text{ abs s}^{-1}$ continuously. To assess reproducibility, five trials were conducted, and t_{ind} was found to be reproducible ± 3 seconds. Over succeeding trials, the strength of the base solution was altered, thus changing the pH_{10} of the resultant solution. Concentrations of species of interest (Al, Mn, SO_4) were varied to measure their effect on t_{ind} .

Conductivity and pH Measurements

Concurrent measurements of conductivity and pH during induction and precipitation were obtained by positioning the pH probe and conductivity probe (Corning Checkmate Modular meter system with conductivity module) in 50 mL of a 10 mM Fe (ferric sulfate) solution, which was rapidly mixed by a magnetic stir plate. At $t = 0$, an equal volume of bicarbonate solution was added. Readings of pH and conductivity were recorded at $t = 0.25$ min, 0.5 min, and every 0.5 min thereafter for a total time of 10 min. To assess reproducibility, repeated trials were conducted with aliquots of the same solutions. For corresponding measurements, the mean standard deviation (sd) for conductivity was 0.021 mS ($n = 140$). The initial pH of the iron

solution was adjusted to pH 2.34 with 6 M nitric acid for all trials. The bicarbonate solutions ranged from 4 mM to 10.5 mM. The induction time (determined visually) was reproducible \pm 0.5 min in 7 trials.

RESULTS AND DISCUSSION

Aluminum and Manganese Effects on Induction Time

Neither Al nor Mn [II] significantly affected induction time in these experiments, as indicated by analysis of variance (ANOVA). The effect of Mn [II] on t_{ind} was examined up to a Mn concentration of 2 mM. At these concentrations, Mn did not have a significant effect on t_{ind} in 1 mM Fe solutions at the $\alpha=0.05$ level. Aluminum was investigated in 1, 5, and 10 mM Fe solutions at Al/Fe ratios up to 10. At these concentrations, Al did not have a significant effect on t_{ind} ($\alpha=0.05$).

Sulfate

The effect of sulfate on t_{ind} for iron concentrations of 1 mM, 5 mM, and 10 mM is shown in Figures 2a, b, and c, respectively. There were statistically significant differences ($P < 0.05$) between all groups of data, as measured by the Students t-Test for closest pairings of groups, except between the $SO_4/Fe = 1.5$ and 3 groups in the 5 mM Fe series and between the $SO_4/Fe = 2.25$ and 3 groups in the 10 mM Fe series.

Table 2. Solution compositions for initial studies of effects of Al, Mn, and sulfate on induction time of 1 mM ferric iron solutions; "low", "med", and "high" refer to the three solution compositions used.

Species	low		med		high	
	mg/L	M	mg/L	M	mg/L	M
Al	0	0.0000	135	0.005	270	0.010
Mn	0	0.0000	55	0.001	110	0.002
SO ₄	144	0.0015	2400	0.025	3840	0.040

Ionic strengths of the various solutions, as calculated with MINTEQA2, were found to range from 0.004 to 0.26 M. When sulfate was held constant (data not shown), there was no correlation between ionic strength and t_{ind} ($R^2 = 0.07$). Thus, any observed effect was not due solely to increased ionic strength.

An inspection of the induction time data suggested a complex relationship among t_{ind} , the sulfate and iron concentrations, and pH. Thus, it was hypothesized that the factors of pH, iron concentration, and sulfate concentration would be significant predictors of induction time. These factors as well as others such as pOH, base/Fe ratio and SO_4/Fe ratio were

- 6 -

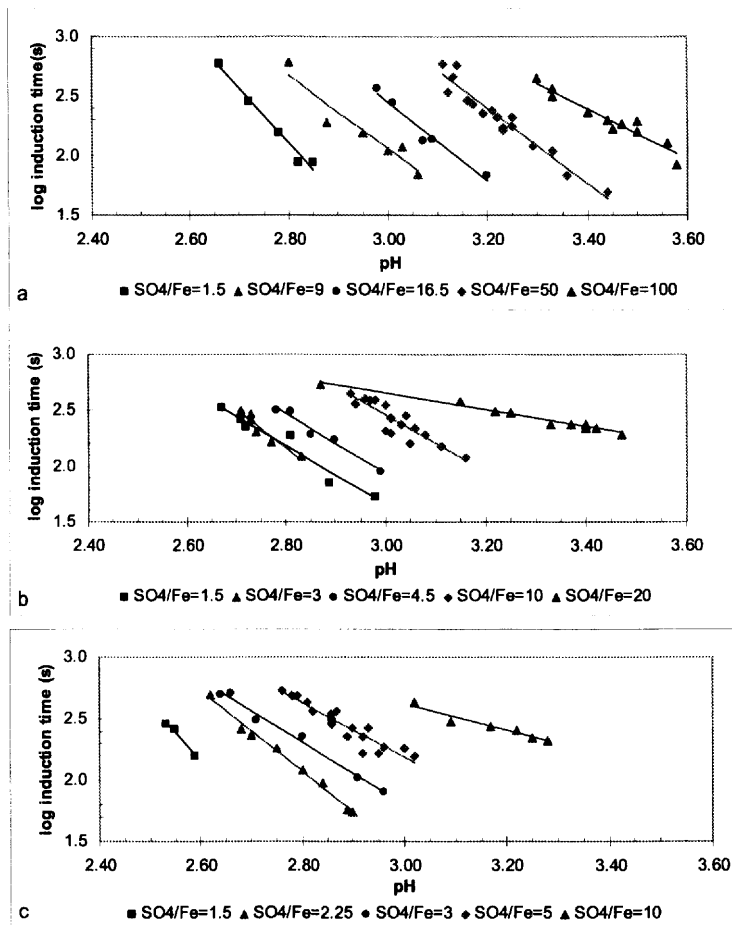


Figure 2. Effect of sulfate on induction time of (a) 1 mM Fe, (b) 5 mM Fe, and (c) 10 mM Fe solutions with different SO₄/Fe ratios. Each data point represents an individual measurement.

evaluated for their ability to predict induction time by means of multiple linear regression. Using Best Subset Regression and Stepwise Multiple Regression, it was found that the factors of pH,

log [Fe], and log [SO₄] were the best predictors of log induction time. The data set was analyzed by the statistical program Minitab Release 10X (Minitab, Inc., State College, PA) for outliers, which exerted a large influence on the regression. After eliminating outliers (10 observations), 123 observations remained. This data set yielded a multiple R² of 0.84 with a high level of significance (P< 0.001). Multiple R² is the Coefficient of Multiple Determination, and indicates the extent to which the combination of factors predicts the dependent variable (Sokal and Rolf, 1995). None of the factors alone produced a significant coefficient of determination (R²). The predictive equation for induction time, with standard errors in parentheses, is:

$$\log t_{ind} = 6.7(\pm 0.30) - 1.29(\pm 0.10)\text{pH} + 0.94(\pm 0.07) \log [\text{SO}_4] - 0.36(\pm 0.05) \log [\text{Fe}] \quad (2)$$

where t_{ind} is induction time in seconds, and [SO₄] and [Fe] are molar concentrations.

When results are plotted against predicted values, a perfect prediction should yield a slope of 1, with a high R². As can be seen in Figure 3, the model provides a good prediction, with a regression line slope of 0.99 and an R² of 0.71. The model was evaluated over the ranges of pH 2.2 to 3.8, [SO₄] from 9 to 100 mM, and [Fe] from 1 to 10 mM.

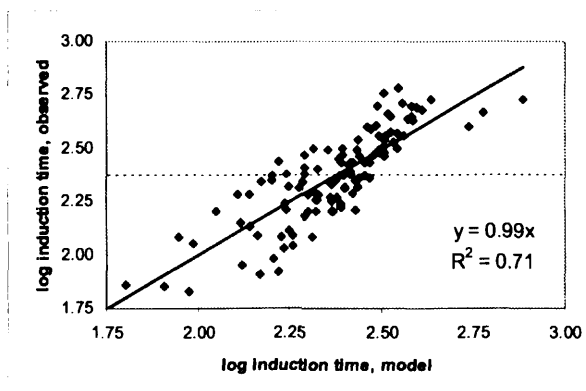


Figure 3. Whole model plot of the multiple regression analysis of induction time data for the precipitation of ferric iron in synthetic AMD after the addition of base. The dashed line represents the mean value for all data points.

Figure 4 shows predicted t_{ind} for a 10 mM Fe solution with pH varied from 2.5 to 4.0, and sulfate concentration varied from 10 to 100 mM. As can be seen, the longest induction times occur in low pH, high-sulfate solutions. It should be noted that the longest observation period in these experiments was 10 min (600 s), and thus the 3-D surface portrayed in Figure 4 extends well beyond the experimental conditions and may not be valid at those extreme induction times.

The induction time is procedure dependent; thus, the procedure used here was chosen to simulate the treatment of AMD in a fluidized bed reactor. If the order of addition of solutions were reversed, a different result would be obtained. It should be noted that the pH recorded (pH_{10}) for each trial was the value observed 10 s after base addition. As discussed later, the pH changed continuously during the induction time and after the appearance of turbidity.

The regression coefficients imply that pH had the largest individual effect on t_{ind} , with an increase in pH decreasing t_{ind} . This is consistent with increased hydrolysis of Fe ions, thus a shortened t_i . Sulfate concentration was the second most important predictor, with increased $[SO_4]$ lengthening t_{ind} , possibly due to increased coverage by sorbed sulfate ions on the HFO surface blocking the attachment of Fe/OH growth units. Bigham et al. (1996) stated that sorbed sulfate appeared to decrease the dissolution rate of these mineral particles, implying reduced reactivity at the surface. Increased $[Fe]$ led to shorter t_{ind} due to a higher degree of supersaturation, resulting in a greater number of nuclei formed and an increased likelihood of effective collisions, thus shortening t_g .

Table 3. Solution composition matrix for studies of the effect of Al and sulfate on induction time at ferric iron concentrations ranging from 1 to 10 mM. Each row under a given iron concentration refers to a given solution composition.

1 mM Fe		5 mM Fe		10 mM Fe	
Ratios		Ratios		Ratios	
Al/Fe	SO ₄ /Fe	Al/Fe	SO ₄ /Fe	Al/Fe	SO ₄ /Fe
0	1.5	0	1.5	0	1.5
0	50	0	10	0	5
0	100	0	20	0	10
5	9	1	3	0.5	2.25
5	50	1	10	0.5	5
10	16.5	2	4.5	1	3
10	50	2	10	1	5
10	100	2	20	1	10

Conductivity and pH Changes During Precipitation

Typical pH and conductivity results are shown in Figures 5a and 5b for a ferric sulfate solution series prepared at $SO_4/Fe = 1.5$. The initial pH of the iron solution was 2.34, its initial conductivity was 2.77 mS, and its initial $[Fe]$ was 10 mM. Since it was only practical to measure changes that occurred relatively slowly, dilute bicarbonate solutions were used, ranging from 4 to 7.5 mM. For practical reasons, the t_{ind} for these trials was determined visually. When t_{ind} was measured instrumentally for certain of the solutions, the times were reasonably close to those determined visually.

No precipitation occurred in the solution prepared with 4 mM bicarbonate, which quickly attained a stable pH of 2.72-2.73 while conductivity decreased at first, reaching a minimum at 5.0 min (time of minimum conductivity = t_{min}), and then slowly increased for the balance of the 10-min observation period. Increased additions of base resulted in exaggerated changes in conductivity and pH during the induction time, corresponding to shorter t_{ind} . Accompanying

shorter t_{ind} was a shorter t_{min} , and a shorter fixed pH plateau followed by a larger drop in pH, a shorter and steeper drop in conductivity followed by a stronger rebound in conductivity. A sharp drop in conductivity was always followed by an increase in conductivity after the initial period. Additional trials (not shown) were consistent with those presented here.

Effect of Sulfate on Conductivity and pH

In other trials, 10 mM Fe solutions and 7.5 mM bicarbonate solutions (base/Fe = 0.75) were prepared using 0%, 50% and 100% synthetic AMD (Figure 6a and b). Higher SO_4/Fe ratio increased the t_{min} , from 1 min in $SO_4/Fe = 1.5$, to 2 min in $SO_4/Fe = 5$. On a proportional basis, the increase in t_{ind} was 3.6 times the increase in t_{min} . The rate of change in conductivity ($\Delta S \text{ min}^{-1}$) was greatest in the low sulfate solution, and decreased with increasing sulfate concentration. Despite different sulfate concentrations, addition of the same amount of base resulted in almost the same pH_{10} . At the same base/Fe ratio, there was a greater decrease in pH in the two lower sulfate solutions than in the highest SO_4/Fe solution. Thus, increased sulfate concentration resulted in diminished

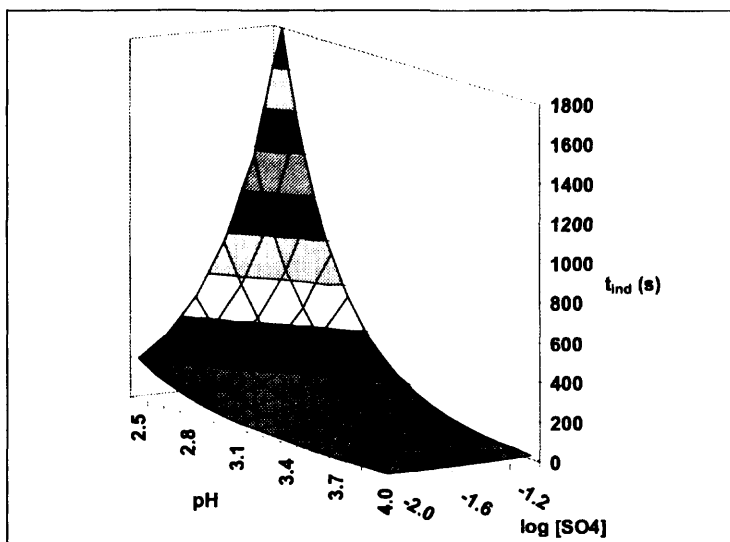
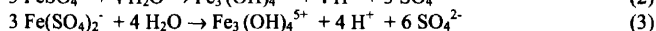


Figure 4. Predicted values for induction time (t_{ind}) in a 10 mM ferric solution with pH varied from 2.5 to 4.0, and sulfate concentration varied from 10 to 100 mM. Note: surface portrayed extends well beyond the experimental conditions and may not be valid at the extreme induction times illustrated.

changes in conductivity and pH during the induction time, which corresponded to longer t_{ind} . Accompanying longer t_{ind} were slightly longer times to minimum conductivity, t_{min} , but t_{ind} and t_{min} did not change at the same rate. Consistent with the van der Woude and de Bruyn (1983) model, an addition of base resulted in a rapid decrease in the charge per iron atom as nucleation occurred, as evidenced by the drop in specific conductivity. It is speculated that the number of nuclei formed, and thus the magnitude of the initial drop in specific conductivity, was a function of the base/Fe addition. Nucleation after this very early phase appeared to be unlikely since the conductivity drop did not continue indefinitely, even though dissolved [Fe] continued to decrease (Diz, 1997). Size distributions reported for HFO precipitates (Buyanov et al., 1972; Dousma and de Bruyn, 1978; Knight and Sylva, 1974) suggest very small particles (perhaps just 50 Fe atoms), as small as 2-3 nm, too small to scatter light. This is consistent with the conductivity reaching a minimum in less than 2 minutes whether precipitation occurred quickly or not at all during the observation period.

It would be reasonable to hypothesize that after these first moments, agglomeration dominated the next phase rather than continued growth of nuclei, but slowed as sizes of about 1 μm were approached. Scanning electron micrographs (Diz and Novak, 1998) and transmission electron micrographs of schwertmannite (Bigham et al., 1996) showed spherical clusters ranging in diameter from about 0.4 to 0.6 μm . Analysis of the precipitates formed in the study by Diz and Novak (1998) found predominately schwertmannite [$\text{Fe}_8\text{O}_8(\text{OH})_6(\text{SO}_4)_2$], which is similar in structure to akaganeite ($\beta\text{-FeOOH}$) (Bigham et al., 1994), but stabilized by sulfate ions instead of chloride.

Other possible explanations for the slow increase in conductivity after t_{min} include: (a) a release of hydrogen ions due to oxolation, as suggested by Dousma and de Bruyn (1976); (b) the release of sorbed sulfate ions as surface area decreased upon aging of the particles; or (c) the hydrolysis of iron as precipitation slowly continued. The first two possibilities are related but unlikely over the short time span considered in this study (minutes rather than months). The third possibility is more likely. As polymerized iron was removed from solution by slow incorporation into HFO surfaces, iron would be released from the complexes FeSO_4^+ and $\text{Fe}(\text{SO}_4)_2^-$ to restore equilibrium. Those iron ions would hydrolyze, releasing H^+ , and slowly become incorporated into the existing HFO surfaces. The overall reactions would be:



Equations 2 and 3 show that a greater number of charged species would be created than would be destroyed as hydrolysis and polymerization of iron proceeded. A release of hydrogen ions would occur as well, which would result in a corresponding drop in pH over time, consistent with the observed results (Figures 5 and 6). The incorporation of polymerized iron into already formed surfaces would be slow, the rate being determined by the saturation factor, π (defined as the ratio of the ion activity product to the solubility product). Since most of the iron was removed during the initial phase, and the release of H^+ lowered the pH, π is decreased; thus the driving force for precipitation would be lower. This was indicated (data not shown) by a slow decline in dissolved [Fe] over the ensuing hours and days (Diz, 1997). It is unlikely that this slow decrease is related to a transformation of the mineral, since a stability study (Bigham et al, 1996) showed that

schwertmannite slowly transformed into goethite over the course of 500 days, with dissolved iron concentration steadily increasing until day 320, and then declining.

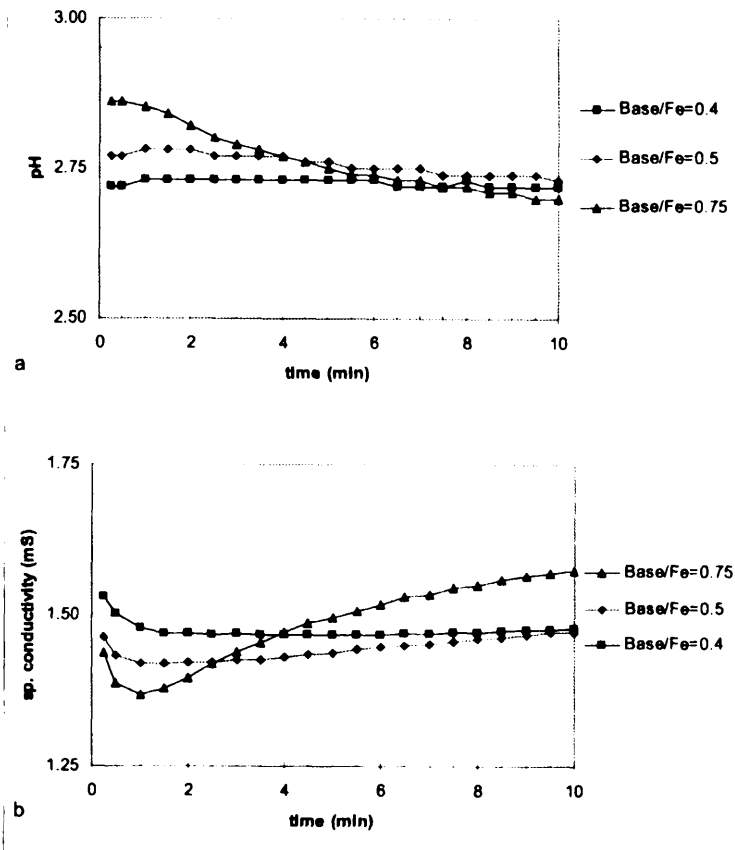


Figure 5. Changes in (a) pH and (b) conductivity during induction and precipitation of ferric sulfate solutions after addition of bicarbonate. Solutions were prepared using equal volumes of 10 mM ferric sulfate with 4, 5, or 7.5 mM bicarbonate at t=0.

- 12 -

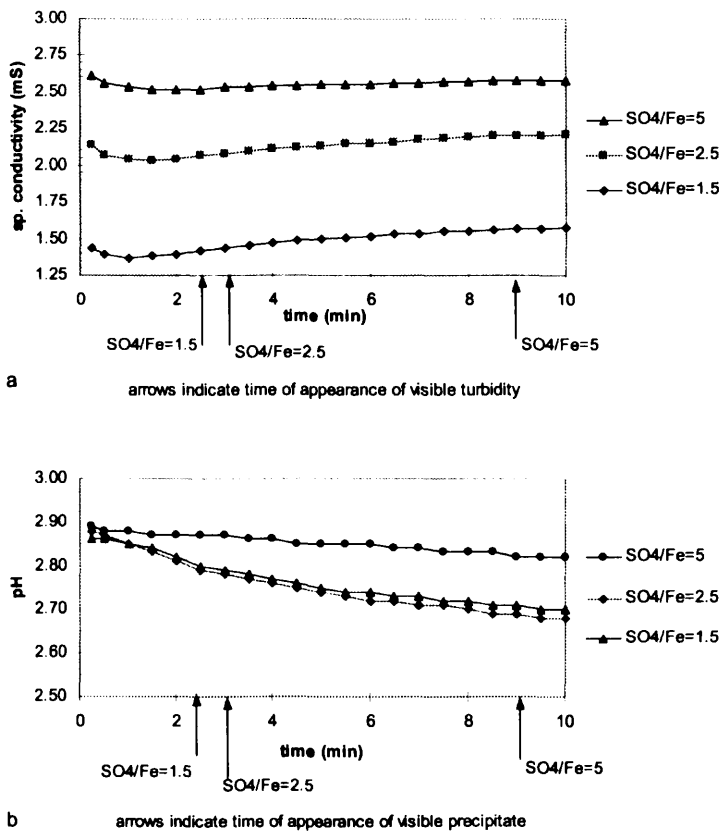


Figure 6. Changes in (a) specific conductivity and (b) pH during induction and precipitation in solutions of different SO₄/Fe ratios; trials were initiated by combining 10 mM iron (ferric sulfate) and 7.5 mM bicarbonate solutions which had both been prepared with deionized water (SO₄/Fe=1.5), 50% AMD (SO₄/Fe=2.5), and 100% AMD (SO₄/Fe=5).

In summary, it was found that within the concentration ranges investigated, Al:Fe and Mn:Fe ratios did not affect HFO induction time. However, induction time for ferric iron could be predicted based on pH and the iron and sulfate concentrations. Thus, design and operation of a

reactor system to precipitate iron can be based primarily on these factors. Also, it was seen that changes in conductivity and pH during induction and precipitation provided some confirmation of the model of van der Woude and de Bruyn (1983), and suggested that fast nucleation is followed by a slower growth period; particles then agglomerated to form precipitates. It seems reasonable to infer that sulfate exerted two effects on HFO growth rates. First, aqueous complexation by sulfate reduced the free ferric ion concentration, and thus lowered π . Second, attachment of polymerized iron to surface sites occupied by sulfate was likely inhibited, thus slowing the growth of iron precipitates.

Acknowledgement: The authors wish to acknowledge the support of the United States Environmental Protection Agency's Science to Achieve Results (STAR) Program for the doctoral fellowship provided to the primary author which enabled this research project.

LITERATURE CITED

- Allison, J.D., D.S. Brown, and K.J. Novo-Gradac. 1991. MINTEQA2/PRODEFA2, a Geochemical Assessment Model for Environmental Systems – Version 3.0 User's Manual: US Environmental Protection Agency Report EPA/600/3-91/021. 106 pp.
- Bigham, J. M., L. Carlson, and E. Murad. 1994. Schwertmannite, a New Iron Oxyhydroxysulphate from Pyhasalmi, Finland, and Other Localities. *Mineralog. Mag.* 58: 641-648.
- Bigham, J. M., U. Schwertmann, S. J. Traina, R. L. Winland, and M. Wolf. 1996. Schwertmannite and the Chemical Modeling of Iron in Acid Sulfate Waters. *Geochim. Cosmochim. Acta*, 60(12): 2111-2121.
- Buyanov, R. A., O. P. Krivornuchko and I. R. Ryzhak, 1972. *Kinet. Katal.* 13: 470.
- Diz, H. R. 1997. Chemical and Biological Treatment of Acid Mine Drainage for the Removal of Heavy Metals and Acidity, Ph.D. dissertation, Virginia Polytechnic Institute and State University, Blacksburg, Virginia.
- Diz, H.R. and J. T. Novak. 1998. A Fluidized Bed for the Removal of Iron From Acid Mine Drainage. *J. of Environ. Engng (ASCE)* 124(8): 701-708.
- Dousma, J. and P.L. de Bruyn. 1976. Hydrolysis-Precipitation Studies of Iron Solutions. I. Model for Hydrolysis and Precipitation from Fe(III) Nitrate Solutions. *J. Colloid Interface Sci.* 56(3): 527-538.
- Dousma, J. and P.L. de Bruyn. 1978. Hydrolysis-Precipitation Studies of Iron Solutions. II. Aging Studies and the Model for Precipitation from Fe(III) Nitrate Solutions. *J. Colloid Interface Sci.* 64(1): 154-170.
- Dousma, J., D. den Ottelander and P.L. de Bruyn. 1979. The Influence of Sulfate Ions on the Formation of Iron (III) Oxides. *J. Inorg. Nucl. Chem.* 41: 1565-1568.

- 14 -

Knight, R. J. and R. N. Sylva. 1974. Precipitation in Hydrolysed Iron (III) Solutions. *J. Inorg. Nucl. Chem.*36: 591-597.

Newman, M. C. and A. W. McIntosh, editors. 1991. *Metal Ecotoxicology, Concepts and Applications*. Lewis Publishers, Chelsea Michigan.

Parfitt, R. L. and R. Smart. 1978. The Mechanism of Sulfate Adsorption on Iron Oxides. *J. Soil Sci. Soc. Am.* 42:48-50.

Sohnel, O. and J. Garside. 1992. *Precipitation: Basic Principles and Industrial Applications*. Butterworth-Heinemann Ltd. Oxford. pp. 391.

Sokal, R. R. and F. J. Rolf. 1995. *Biometry: The Principles and Practice of Statistics in Biological Research*, 3rd Edition. W. H. Freeman and Company. New York.

Stumm, W. and J. J. Morgan. 1981. *Aquatic Chemistry, An Introduction Emphasizing Chemical Equilibria in Natural Waters*, 2nd Edition. John Wiley & Sons, Inc., New York.

USEPA. 1976. Development Document for Interim Final Effluent Limitations Guidelines and New Source Performance Standards for the Coal Mining Point Source Category. EPA 440/1-76/057a, 288 pp.

van der Woude, J.H.A. and P.L. de Bruyn. 1983. Formation of Colloidal Dispersions From Supersaturated Iron (III) Nitrate Solutions. I. Precipitation of Amorphous Iron.